ELSEVIER

Applied Ocean Research 26 (2004) 154–161

Applied Ocean Research

www.elsevier.com/locate/apor

Response cumulant analysis of a linear oscillator driven by Morison force

X.Y. Zheng*, C.Y. Liaw

Department of Civil Engineering, National University of Singapore 117576, Singapore

Received 13 December 2003; revised 20 December 2004; accepted 11 January 2005
Available online 9 April 2005

Abstract

A frequency-domain cumulant spectral analysis method is developed in this study to estimate the higher-order statistics of the linear oscillator responses driven by Morison wave force. The fourth-order cumulant function of the nonlinear drag force is formulated in terms of the autocorrelation functions of water particle velocity. Price's theorem is applied to evaluate the associated higher-order joint moments. Three-dimensional Fourier Transforms are employed to obtain the trispectra of Morison force and oscillator responses. The estimated force and response kurtosis are in good agreement with those obtained from time-domain simulations; while the proposed method is found to be much more efficient. The numerical results also show that the drag force cubicization based on the least square approximation results in an overestimation of the kurtosis values; in addition, it is necessary to include the joint moments of order higher than eighth.

Keywords: Morison force; Drag force cubicization; Fourth-order cumulant function; Trispectrum; Kurtosis; Correlation function; Three-dimensional FFT; Price's theorem

1. Introduction

It is known that due to the nonlinearities of wave forces, the dynamic structural responses of an offshore system tend to be non-Gaussian in stochastic ocean waves, even if linear waves are assumed and the structural nonlinearity is not considered. Liaw and Zheng [1] reported that for fixed offshore structures, like jack-up and jacket platforms, the nonlinear effects mainly arise from two Morison-type wave forces: the distributed Morison force and the wave elevation induced inundation force. Both forces lead to significant super-harmonic phenomena [2–5]. In the absence of current, the power spectra of these two wave forces exhibit obvious peaks respectively at triple and twice the peak wave frequency (ω_p). Since the natural frequency of a fixed offshore platform (ω_n) is usually higher than ω_p and lower than $4\omega_p$, the structural responses incurred by these two forces can be rather significant.

The non-Gaussian description of the structural response manifests itself on how well the probability density distribution (PDF) is fitted in the tail regions. It has been shown [6,7] that the quasi-static response of a linear system driven by Morison force follows the Pierson-Holmes type distribution of the force [8]. This is however true only for a very rigid structure with ω_n much higher than ω_p [9]. If ω_n is lower than $4\omega_p$, an approximate but reasonable PDF of the response can still be obtainable based on the first four statistical moments of the response [10]. Nonetheless, estimation of higher-order moments, like kurtosis, is not straightforward. To obtain the response moments, stochastic analysis can be conducted, in either time domain or frequency domain. In time-domain analysis, Monte Carlo simulation based on spectral representation method is commonly applied. To acquire converged higher-order statistics, the computing time could be excessive [11] because of large number of frequency components involved and sample functions employed in simulations.

On the other hand, stochastic analysis in the frequency domain can be an efficient alternative. The Volterra series-based model has been used to estimate the associated cumulant spectra (power spectrum, bispectrum and trispectrum) of the responses of offshore structures [12–14]. The application of Volterra model demands that the nonlinear Morison drag term be approximated by polynomials for determining the transfer functions. With increasing polynomial degrees, such a model has two drawbacks that significantly reduce its applicability: dramatic increase of

* Corresponding author. Tel.: +65 6874 1270; fax: +65 6779 1635.
E-mail address: cvezxy@nus.edu.sg (X.Y. Zheng).

0141-1187/$ - see front matter © 2005 Elsevier Ltd. All rights reserved.
doi:10.1016/j.apor.2005.01.001

complexity in deriving higher-order spectra [15] and, rapidly growing numerical efforts in estimating the higher-order statistics that involves multi-dimensional integrals [11,15].

Another frequency-domain approach, which is based on the correlation functions of wave kinematics, was also developed to obtain the desired cumulant spectra of response. For a linear time-invariant (LTI) system, the relationship of nth-order cumulant spectra of the input (*wave force*) and the output (*structural response*) has been established [16]; and we know that most fixed offshore structures can be idealized as LTI vibration systems [11]. Therefore, the major task is to obtain the cumulant spectra of wave force.

Power spectral analysis of Morison wave loading based on correlation functions has been reported in some works. In the absence of current, Borgman [17] used Price's theorem [18] to derive the autocorrelation function of the Morison drag force in terms of the autocorrelation of water particle velocity. The corresponding power spectrum could be evaluated by multi-convolutions or Fourier Transform. In the presence of current, fourth-degree drag approximation has been utilized [3] to obtain the autocorrelation of Morison force. The correlation function based scheme was also extended to higher-order spectral analysis [9,19,20]. Hu and Lutes [19] derived the fourth-order cumulant function of Morison drag force using power series expansion, which involved the product of up to four correlation functions of velocity, i.e. the eighth-order joint moment. Utilizing cubic polynomial fit of the drag based on the least squares approximation (LSA), Hu and Dixit [20] obtained the similar cumulant function of drag. The authors noticed that the drag cumulant functions obtained were actually truncated without including 10th- and 12th-order joint moments of the water particle velocity; moreover, the drag trispectrum and response kurtosis were respectively evaluated using 1D FFT and multi-fold integration, instead of the more efficient triple FFT. Also, as pointed out by Bouyssy et al. [11], Tognarelli and Kareem [21], if LSA method is applied, the drag cubicization fails to capture the proper response kurtosis; unless a fifth or higher-degree approximation is introduced. As a result, the difficulties in both mathematical manipulation and numerical computation will increase significantly. However, if the moment-based approximation (MBA) is employed for drag cubicization, the kurtosis values of force and response could be preserved reasonably [14,22,23]. This study aims to develop a more convenient and accurate method for cumulant spectral analysis of the Morison wave force.

2. Input–output spectral relationship

The dynamic motion of a LTI oscillator driven by the Morison force is governed by the following equation:

$$m\ddot{y} + c\dot{y} + ky = f \tag{1}$$

where m, c and k are the oscillator mass, damping and stiffness, respectively; y is the displacement; f is the Morison force per unit length describing the in-line force impinging on a stationary and slender vertical cylinder:

$$f(z,t) = f_{\mathrm{I}} + f_{\mathrm{D}} \tag{2}$$

where f_{I} and f_{D} are, respectively, the inertia and drag forces, i.e.:

$$f_{\mathrm{I}} = C_{\mathrm{M}} A_{\mathrm{I}} \dot{u} = k_{\mathrm{I}} \dot{u} \tag{3}$$

$$f_{\mathrm{D}} = C_{\mathrm{D}} A_{\mathrm{D}} u|u| = k_{\mathrm{D}} u|u| \tag{4}$$

where $A_{\mathrm{I}} = \pi\rho D_{\mathrm{eq}}^2/4$ and $A_{\mathrm{D}} = \rho D_{\mathrm{eq}}/2$; ρ, the water density; D_{eq}, the equivalent diameter of the cylinder; C_{M} and C_{D}, the inertia and drag coefficients; u and $\dot{u}$ are the horizontal water particle velocity and acceleration, respectively, $u = u(z,t)$ and $\dot{u} = \partial u/\partial t$; z, the submerged position measured from the still water level (SWL), positive upward. To include wave-structure interactions, the modified Morison equation should be used. Considering the structural velocity of a fixed rig is usually much smaller than the water particle velocity [3,4], the modified drag term can then be approximated as:

$$f_{\mathrm{D}} = k_{\mathrm{D}}(u - \dot{y})|u - \dot{y}| \approx k_{\mathrm{D}} u|u| - 2\dot{y}|u| \tag{5}$$

The term $2\dot{y}|u|$ incurs a fluid damping, the effect of which can be taken into account [3,4,9] by adjusting the system damping in Eq. (1). This allows us to retain the zero-memory term in Eq. (4). In addition, to account for the effects of current, velocity u should be replaced by $u+c$; c is the current speed. Based on drag force cubicization, it has been found that [24] the existence of current will soften the nonlinearity of drag force by reducing the force kurtosis. The effects of current on variance and higher-order statistics of structural response have been also investigated [3,13]. This study will not include current effects and the focus is on the interested cumulant spectral analysis.

In the spectral analysis of a LTI system, the relationship of the nth-order ($n \geq 2$) cumulant spectra $S(\omega_1,\ldots,\omega_{n-1})$ of the stationary input f and output y is given as [16]:

$$\begin{aligned} &S_y(\omega_1, \omega_2, \ldots, \omega_{n-1}) \\ &\quad = H_{fy}(\omega_1) H_{fy}(\omega_2) \cdots H_{fy}(\omega_{n-1}) H_{fy}^*(\omega_1 + \omega_2 + \ldots \\ &\qquad + \omega_{n-1}) S_f(\omega_1, \omega_2, \ldots, \omega_{n-1}) \end{aligned} \tag{6}$$

where $H_{fy}(\omega)$ is the linear transfer function from f to y:

$$H_{fy}(\omega) = \frac{1}{m(\omega_n^2 - \omega^2 + 2i\xi\omega_n\omega)} \tag{7}$$

with the natural frequency $\omega_n = \sqrt{k/m}$, damping ratio $\xi = c/2m\omega$ and $i = \sqrt{-1}$. Obviously that $S_y(\omega_1, \omega_2, \ldots, \omega_{n-1})$ depends on $S_f(\omega_1, \omega_2, \ldots, \omega_{n-1})$, which is available through the $(n-1)$-dimensional Fourier Transform of the nth-order

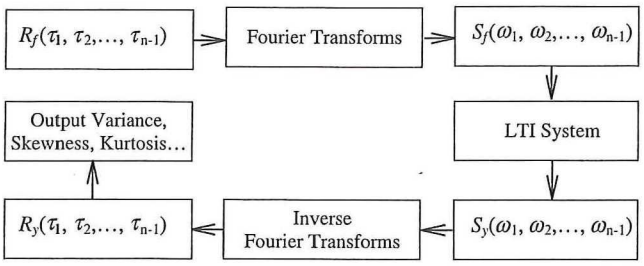

Fig. 1. Cumulant spectral analysis of a LTI system.

cumulant functions of the force [16]:

$$S_f(\omega_1, \omega_2, \ldots, \omega_{n-1}) = \int \cdots \int_{-\infty}^{\infty} R_f(\tau_1, \tau_2, \ldots, \tau_{n-1}) \exp\{-j(\omega_1\tau_1 + \omega_2\tau_2 + \cdots + \omega_{n-1}\tau_{n-1})\} \mathrm{d}\tau_1 \, \mathrm{d}\tau_2 \ldots \mathrm{d}\tau_{n-1} \quad (8)$$

Analogously, if $S_y(\omega_1, \omega_2, \ldots, \omega_{n-1})$ is known, the nth-order cumulant functions of displacement can be estimated through the $(n-1)$-dimensional inverse Fourier Transform:

$$R_y(\tau_1, \tau_2, \cdots, \tau_{n-1}) = \frac{1}{(2\pi)^{n-1}} \int \int \cdots \int_{-\infty}^{\infty} S_y(\omega_1, \omega_2, \ldots, \omega_{n-1}) \times \exp\left\{j(\omega_1\tau_1 + \omega_2\tau_2 + \cdots + \omega_{n-1}\tau_{n-1})\right\} \mathrm{d}\omega_1 \mathrm{d}\omega_2 \ldots \mathrm{d}\omega_{n-1} \quad (9)$$

By choosing $n=2,3,4$, $S(\omega_1, \omega_2, \ldots, \omega_{n-1})$ represents the power-spectrum, bispectrum and trispectrum, respectively, and $R(\tau_1, \tau_2, \ldots, \tau_{n-1})$ represents the autocorrelation function, third- and fourth-order cumulant functions. Setting $\tau_1=\tau_2=\tau_3=0$, the skewness and kurtosis are obtained in the following normalized form:

$$\kappa_3 = \frac{R(0,0)}{R^{3/2}(0)}, \kappa_4 = \frac{R(0,0,0)}{R^2(0)} \quad (10)$$

Fig. 1 depicts the procedures in cumulant spectral analysis of a LTI system. The critical issue here is how to formulate the input cumulant functions.

3. Drag approximation and autocorrelation of f

The wave elevation, $\eta(t)$, at a fixed location can be considered as a Gaussian process of a zero mean. Based on linear wave theory, the linear transfer functions from η to u and $\dot{u}$ are:

$$H_{\eta u}(z, \omega) = \omega r(z) \quad (11)$$

$$H_{\eta \dot{u}}(z, \omega) = i\omega^2 r(z) = i\omega H_{\eta u}(z, \omega) \quad (12)$$

where $r(z) = \cosh k(z+d)/\sinh kd$. The wave number k is related to the wave frequency ω by the dispersion function $\omega^2 = kg \tanh kd$; g is the gravity constant. Note that u and $\dot{u}$ preserve the Gaussian properties because of the linear transformations. Their respective spectra can be obtained from a given wave spectrum $S_{\eta\eta}(\omega)$:

$$\begin{cases} S_{uu}(z, \omega) = S_{\eta\eta}(\omega)|H_{\eta u}(z, \omega)|^2 \\ S_{\dot{u}\dot{u}}(z, \omega) = S_{\eta\eta}(\omega)|H_{\eta \dot{u}}(z, \omega)|^2 \end{cases} \quad (13)$$

Under the joint-Gaussian assumption, random variables $\dot{u}(z, t)$ and $u(z,t)$ at the same time point t are independent [7, 8]. In this study, the random processes $\dot{u}(z, t)$ and $u(z,t)$ are assumed to be independent. Hence, f_{I} and f_{D} are also independent, which allows the cumulant spectra, including the power, bi- and tri-spectra, of f to be written as [16]:

$$S_f(\omega_1, \omega_2, \ldots, \omega_{n-1}) = S_{f_{\mathrm{I}}}(\omega_1, \omega_2, \ldots, \omega_{n-1}) + S_{f_{\mathrm{D}}}(\omega_1, \omega_2, \ldots, \omega_{n-1}) \quad (14)$$

and cumulant functions:

$$R_f(\tau_1, \tau_2, \ldots, \tau_{n-1}) = R_{f_{\mathrm{I}}}(\tau_1, \tau_2, \ldots, \tau_{n-1}) + R_{f_{\mathrm{D}}}(\tau_1, \tau_2, \ldots, \tau_{n-1}) \quad (15)$$

For brevity, the Morison force f treated hereafter is the one acting at SWL, i.e. $z=0$.

Borgman [17] derived the closed-form and complete expression of the autocorrelation of f_{D} in a series expansion. In numerical computation, the polynomial approximation of the drag term $u|u|$ is more often accepted for derivation [3,25]. Let $x=u/\sigma_u$, the x follows the standard Gaussian distribution with the corresponding PDF expressed as:

$$p(x) = \frac{1}{\sqrt{2\pi}} \mathrm{e}^{-(x^2/2)} \quad (16)$$

The cubic approximation of the drag based on LSA method is [25]:

$$r = x|x| \approx \sqrt{\frac{2}{\pi}}\left(x + \frac{1}{3}x^3\right) \quad (17)$$

and that based on MBA method is [22]:

$$r = 1.0079x + 0.2142x^3 \quad (18)$$

The nth-order moment of r can be estimated [3,24] based on $p(x)$ in Eq. (16), e.g.,:

$$m_n^r = \int (x|x|)^n p(x) \, \mathrm{d}x \quad (19)$$

For odd n, all moments of r vanish and the solutions for even n are:

$$m_n^r = (2n-1)(2n-3)\cdots 1 \quad (20)$$

The variance is equal to the 2nd-order moment and kurtosis is defined as [16]:

$$\kappa_r = \frac{\mathrm{cm}_4^r}{\sigma_r^4} - 3 \quad (21)$$

where cm_4^r is the fourth-order central moment of r, which in this case is:

$$\mathrm{cm}_4^r = m_4^r \quad (22)$$

The kurtosis defined here and in Eq. (10) is also termed coefficient of excess or kurtosis excess in some books. For a Gaussian process, it is equal to zero and for the drag term $r=x|x|$, it is equal to 8(2/3) that will be considered as an important criterion for time simulations later in this study. The autocorrelation of f based on drag cubicization is [2]:

$$R_f(\tau) = R_{f_I}(\tau) + R_{f_D}(\tau) \tag{23}$$

The autocorrelations of the inertia and drag parts on the RHS are [26]:

$$R_{f_I}(\tau) = k_I^2 R_{\dot{u}\dot{u}}(\tau) \tag{24}$$

$$R_{f_D}(\tau) = k_D^2[(c_1 + 3c_3\sigma_u^2)^2 R_{uu}(\tau) + 6c_3^2 R_{uu}^3(\tau)] \tag{25}$$

where $c_1=a_1\sigma_u$ and $c_3=a_3\sigma_u$; a_1 and a_3 are the linear and cubic polynomial coefficients in Eqs. (17) and (18). It is obvious that $R_f(\tau)$ involves only the autocorrelations of u and $\dot{u}$, which can be easily obtained through the inverse Fourier Transforms of the corresponding power spectra:

$$\begin{cases} R_{uu}(\tau) = \dfrac{1}{2\pi}\displaystyle\int S_{uu}(\omega)e^{i\omega\tau}\,d\omega \\ R_{\dot{u}\dot{u}}(\tau) = \dfrac{1}{2\pi}\displaystyle\int S_{\dot{u}\dot{u}}(\omega)e^{i\omega\tau}\,d\omega \end{cases} \tag{26}$$

The power spectrum of Morison force is then:

$$S_f(\omega) = \int R_f(\tau)e^{-i\omega\tau}d\tau \tag{27}$$

According to Eq. (6), the power spectrum of the oscillator response is simply:

$$S_y(\omega) = |H_{fy}(\omega)|^2 S_f(\omega) \tag{28}$$

4. Fourth-order cumulant function of f

Since both the inertia and drag forces are odd-degree functions of Gaussian wave kinematics, the odd-order statistics, including mean and skewness, of Morison force and the induced oscillator response are zeros. One only needs to be concerned about the fourth-order cumulant function for kurtosis estimation. Considering that the inertia force is simply a linear function of $\dot{u}$, it is Gaussian and its cumulant functions of order 3 and 4 vanish [16]. Hence, according to Eq. (15), the 4th-order cumulant function of f is only attributable to the drag part:

$$R_f(\tau_1,\tau_2,\tau_3) = R_{f_D}(\tau_1,\tau_2,\tau_3) \tag{29}$$

Let $u_1=u(t)$, $u_2=u(t+\tau_1)$, $u_3=u(t+\tau_2)$, $u_4=u(t+\tau_3)$ and $x_1=f_D(t)=k_D(c_1u(t)+c_3u^3(t))$, $x_2=f_D(t+\tau_1)$, $x_3=f_D(t+\tau_2)$, $x_4=f_D(t+\tau_3)$, recall that f_D has a zero mean, $R_{f_D}(\tau_1,\tau_2,\tau_3)$ is expressible in terms of its 2nd- and 4th-order moment functions [16]:

$$R_{f_D}(\tau_1,\tau_2,\tau_3) = R[x_1,x_2,x_3,x_4] = E[x_1x_2x_3x_4] - R_{\prod} \tag{30}$$

where

$$R_{\prod} = E[x_1x_2]E[x_3x_4] + E[x_1x_3]E[x_2x_4] + E[x_1x_4]E[x_2x_3] \tag{31}$$

Obviously R_Π involves only double convolutions of the autocorrelation of f_D and can be obtained straightforwardly. For instance, the first term on the RHS is $E[x_1x_2]E[x_3x_4]=R_{f_D}(\tau_1)R_{f_D}(\tau_3-\tau_2)$, where $R_{f_D}(\tau)$ is available in Eq. (25). The problem reduces to finding the complicated fourth-order moment function of f_D in an expectation form:

$$\begin{aligned} m_4^{f_D} &= E[x_1x_2x_3x_4] = k_D^4E[(c_1u_1 + c_3u_1^3)(c_1u_2 + c_3u_2^3) \\ &\quad \times (c_1u_3 + c_3u_3^3)(c_1u_4 + c_3u_4^3)] \end{aligned} \tag{32}$$

which consists of the joint moments of u with even orders from fourth to twelfth. The 4th-order moment comes only from the linear drag term, i.e.

$$E4 = k_D^4c_1^4E[u_1u_2u_3u_4] \tag{33}$$

while the 12th-order moment consists of only the cubic drag terms, i.e.

$$E12 = k_D^4c_3^4E[u_1^3u_2^3u_3^3u_4^3] \tag{34}$$

The 6th-, 8th- and 10th-order moments arise from the cross effects of linear and cubic drag terms. The 6th-order moments $E6$ have four different forms and one of them is [27]:

$$E6 = k_D^4c_1^3c_3E[u_1u_2u_3u_4^3] \tag{35}$$

The 8th-order moments $E8$ have six different forms and one of them is:

$$E8_A = k_D^4c_1^2c_3^2E[u_1u_2u_3^3u_4^3] \tag{36}$$

The 10th-order moments $E10$ also have four different forms and one of them is:

$$E10_A = k_D^4c_1c_3^3E[u_1u_2^3u_3^3u_4^3] \tag{37}$$

Since the velocities u_i ($i=1,2,3,4$) are jointly Gaussian, Price's theorem [18] is suitable for decomposing the above higher-order joint moments into products of the autocorrelation $R_{uu}(\tau)$. The most complicated joint moment $E12$ in Eq. (34) was found to consist of as many as $11\cdot9\cdot7\cdot5\cdot3\cdot1=10395$ products and was actually the main stumbling-block of previous studies [9,19]. Fortunately, because u has only four distinct time lags (t, $t+\tau_1$, $t+\tau_2$, $t+\tau_3$), most of the 10395 products are repetitive and $E12$ can be reduced to a sum of much fewer basic products. Therefore, two algorithms have been developed: one is a recursive algorithm to perform the complete moment decomposition according to Price's theorem; the other is for moment condensation [27]. Table 1 lists the condensed 47 non-repetitive products of $E12$. The first row, e.g., symbolizes such a product of

Table 1
Non-repetitive products of $E12$

Products	Repeating times
1 1 1 2 2 2 3 3 3 4 4 4	81
1 1 1 2 2 2 3 4 3 4 3 4	54
1 1 1 2 2 3 2 3 3 4 4 4	162
1 1 1 2 2 3 2 4 3 3 4 4	162
1 1 1 2 2 3 2 4 3 4 3 4	324
1 1 1 2 2 4 2 4 3 3 3 4	162
1 1 1 3 2 2 2 3 3 4 4 4	162
1 1 1 3 2 2 2 4 3 3 4 4	81
1 1 1 3 2 2 2 4 3 4 3 4	162
1 1 1 3 2 3 2 3 2 4 4 4	162
1 1 1 3 2 3 2 4 2 4 3 4	324
1 1 1 3 2 4 2 4 2 4 3 3	54
1 1 1 4 2 2 2 3 3 3 4 4	81
1 1 1 4 2 2 2 3 3 4 3 4	162
1 1 1 4 2 2 2 4 3 3 3 4	162
1 1 1 4 2 3 2 3 2 3 4 4	54
1 1 1 4 2 3 2 3 2 4 3 4	324
1 1 1 4 2 3 2 4 2 4 3 3	162
1 2 1 2 1 2 3 3 3 4 4 4	54
1 2 1 2 1 2 3 4 3 4 3 4	36
1 2 1 2 1 3 2 3 3 4 4 4	324
1 2 1 2 1 3 2 4 3 3 4 4	162
1 2 1 2 1 3 2 4 3 4 3 4	324
1 2 1 2 1 4 2 3 3 3 4 4	162
1 2 1 2 1 4 2 3 3 4 3 4	324
1 2 1 2 1 4 2 4 3 3 3 4	324
1 2 1 3 1 3 2 2 3 4 4 4	162
1 2 1 3 1 3 2 3 2 4 4 4	324
1 2 1 3 1 3 2 4 2 4 3 4	324
1 2 1 3 1 4 2 2 3 3 4 4	162
1 2 1 3 1 4 2 2 3 4 3 4	324
1 2 1 3 1 4 2 3 2 3 4 4	324
1 2 1 3 1 4 2 3 2 4 3 4	1296
1 2 1 3 1 4 2 4 2 4 3 3	324
1 2 1 4 1 4 2 2 3 3 3 4	162
1 2 1 4 1 4 2 3 2 3 3 4	324
1 2 1 4 1 4 2 3 2 4 3 3	324
1 3 1 3 1 3 2 2 2 4 4 4	54
1 3 1 3 1 3 2 4 2 4 2 4	36
1 3 1 3 1 4 2 2 2 3 4 4	162
1 3 1 3 1 4 2 2 2 4 3 4	324
1 3 1 3 1 4 2 3 2 4 2 4	324
1 3 1 4 1 4 2 2 2 3 3 4	324
1 3 1 4 1 4 2 2 2 4 3 3	162
1 3 1 4 1 4 2 3 2 3 2 4	324
1 4 1 4 1 4 2 2 2 3 3 3	54
1 4 1 4 1 4 2 3 2 3 2 3	36

correlation functions:

$$E12_{1st} = 81R_{11}R_{12}R_{22}R_{33}R_{34}R_{44} \tag{38}$$

where $R_{11}=R_{22}=R_{33}=R_{44}=R_{uu}(0)=\sigma_u^2$, $R_{12}=R_{uu}(\tau_1)$, $R_{13}=R_{uu}(\tau_2)$, $R_{14}=R_{uu}(\tau_3)$, $R_{23}=R_{uu}(\tau_2-\tau_1)$, $R_{24}=R_{uu}(\tau_3-\tau_1)$, $R_{34}=R_{uu}(\tau_3-\tau_2)$. Eq. (38) implies that, like $R_{\prod}$ in Eq. (31), $E12$ and other lower-order joint moments ($E6$, $E8$, $E10$) can all be evaluated based on $R_{uu}(\tau)$. The 4th-order cumulant function of f_D in Eq. (30)

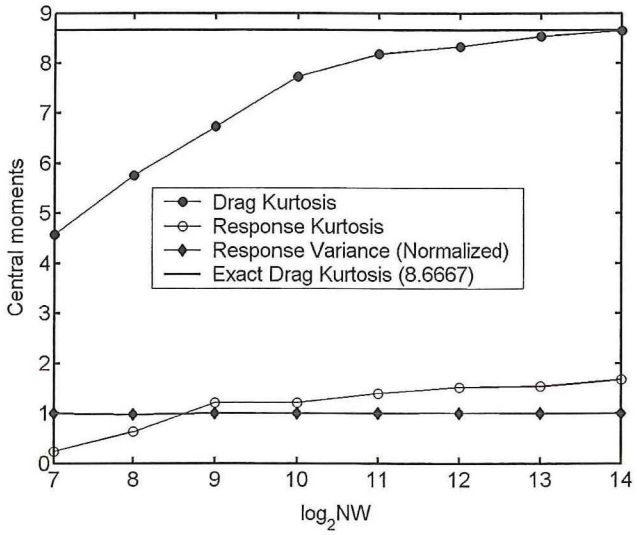

Fig. 2. Effects of frequency number on simulated moments.

can then be rewritten as:

$$R_{f_D}(\tau_1,\tau_2,\tau_3) = E4 + E6 + E8 + E10 + E12 - R_{\prod} \tag{39}$$

Setting τ_1, τ_2 and τ_3 to be zeros, the kurtosis of f_D and f are:

$$\kappa_4^{f_D} = \frac{R_{f_D}(0,0,0)}{R_{f_D}^2(0)}, \quad \kappa_4^{f} = \frac{R_{f_D}(0,0,0)}{[R_{f_D}(0)+R_{f_I}(0)]^2} \tag{40}$$

Following the procedures described in Fig. 1, tripectrum of Morison force $S_{f_D}(\omega_1,\omega_2,\omega_3)$ is obtained by the triple Fourier transform of $R_{f_D}(\tau_1,\tau_2,\tau_3)$; and response trispectrum $S_y(\omega_1,\omega_2,\omega_3)$ is evaluated according to the input–output relationship in Eq. (6); then, using the triple inverse Fourier transform, we have the fourth-order response cumulant function $R_y(\tau_1,\tau_2,\tau_3)$ and the corresponding kurtosis is:

$$\kappa_4^{y} = \frac{R_y(0,0,0)}{R_y^2(0)} \tag{41}$$

where response variance $R_y(0)$ can be evaluated from the power spectrum in Eq. (28).

5. Numerical evaluation of $R_f(\tau_1,\tau_2,\tau_3)$

The power spectra of wave force can be numerically evaluated with negligible computer time [26], in that there is only one time shift τ involved and 1-D FFT is needed. However, the foregoing cumulant spectral analysis involves a triple FFT of $R_f(\tau_1,\tau_2,\tau_3)$ which in its discrete form is a cube of the size NP×NP×NP (NP: number of FFT points), with the three dimensions corresponding to τ_1, τ_2 and τ_3. Thus, if NP is large, the numerical effort is significant for generating $R_f(\tau_1,\tau_2,\tau_3)$ and implementing the triple FFT. In

addition, the computer memory is another problem of concern because both $R_f(\tau_1,\tau_2,\tau_3)$ and trispectrum are huge matrices. To formulate $R_f(\tau_1,\tau_2,\tau_3)$, loops about τ_1, τ_2 and τ_3 should be avoided. A 'page-by-page' scheme was proposed [27] to do the loop just about τ_3 with the 'page', a 2-D matrix about τ_1 and τ_2, formed using efficient matrix multiplications. Such a scheme not only saves numerous numerical efforts but makes coding easier. Another scheme [27] to facilitate computation was based on symmetries of $R_f(\tau_1,\tau_2,\tau_3)$ itself-only half of the pages need to be produced.

6. Example and results

The stochastic displacement response of a LTI oscillator (unit length) excited by the Morison force at SWL is investigated. Ocean wave conditions are considered by employing a JONSWAP spectrum [28] with the following parameters: significant wave height of 9.9 m; peak wave frequency ω_p of 0.521 rad/s, peak enhancement factor γ of 3.3 and water depth of 30 m. Inertia and drag coefficients for calculating Morison force are, respectively, 1.78 and 4.0. The vibration system of oscillator has a damping ratio of 0.07, mass 1000 kg and natural frequency 1.422 rad/s—a value close to $3\omega_p$, indicating the existence of third-order super-harmonic responses.

6.1. Time-domain simulation

In time-domain simulations, the standard spectral representation method is applied to obtain time records of the inertia, drag and local Morison force. The exact expression of the drag is adopted without polynomial approximation. The induced oscillator response is calculated using the linear acceleration time-integration method.

To acquire converged statistical moments, as many as 120 sample functions [11] are simulated. Each simulation corresponds to a wave storm lasting for 3 h, as recommended by SNAME [28]. Considering that the convergence of higher-order moments is also dependent on the number of frequency components (NW) in spectral discretization, Fig. 2 plots drag kurtosis, response kurtosis and variance versus $\log_2$NW. The value of variance is normalized by the one corresponding to the largest NW $= 2^{14} = 16384$. It can be easily seen that there is little variation of variance with NW; even a small NW $= 2^7 = 128$ is able to make a good estimation of the variance. However, both drag and response kurtosis increase with NW. The drag kurtosis approaches the exact value 8.6667 and the response kurtosis becomes stable when 16384 harmonic components are used. The value, 8.6667, may act as an important criterion to test the effectiveness of simulations: a reasonable response kurtosis demands that the drag kurtosis be simulated close to 8.6667. On the other hand, to meet this criterion means excessive computation time [11].

Table 2 presents the simulated variances and fourth-order cumulants (underlined) of forces f_I, f_D and f, for NW $=$ 16384. The cumulants of f are found very close to the sum of the inertia and drag cumulants and the fourth-order cumulant of f is almost identical to that of f_D, which to some extent supports the assumption that u and $\dot{u}$ are independent.

6.2. Cumulant spectral analysis

The kurtosis of oscillator response is also evaluated using the proposed cumulant spectral analysis method, with the computing time around 9 min for as many as 256 FFT points. Table 2 shows the variance and kurtosis values of wave forces f_I, f_D and f. The response variance and kurtosis are displayed in Table 3. A comparison between MBA and LSA cubicization is made based on these statistics. In these two tables, frequency-domain results are further compared with those of time simulations. To investigate the contributions by joint moments $E10$ and $E12$, the kurtosis values of drag force, Morison force and response without these two moments included are shown in brackets. The following observations can be made:

(1) The variance and kurtosis produced in the frequency-domain approach, based on MBA drag cubicization, tally well with those from time simulations. The relative difference of the kurtosis, for both Morison force and response, is less than 2%. For variance, the difference is even smaller. However, there is a large difference in

Table 2
Variance and kurtosis of wave forces

	Approach	Inertia f_I	Drag f_D	Morison f
Variance	MBA	$1.9956\times10^{+002}$	$8.1219\times10^{+002}$	$1.0118\times10^{+003}$
	LSA	$1.9965\times10^{+002}$	$8.5420\times10^{+002}$	$1.0539\times10^{+003}$
	Simulation	$2.0026\times10^{+002}$	$8.1155\times10^{+002}$	$1.0118\times10^{+003}$
Kurtosis	MBA	0	8.6225 (2.0539)	5.5565 (1.3522)
	LSA	0	$1.3515\times10^{+001}$	9.0097
	Simulation	9.9161×10^{-004}	8.6544	5.5708
		$4.2227\times10^{+001}$	$5.7358\times10^{+006}$	$5.7384\times10^{+006}$

Table 3
Variance and kurtosis of response

	Approach	Oscillator
Variance (m^2)	MBA	$9.3238\times10^{+002}$
	LSA	$9.6542\times10^{+002}$
	Simulation	$9.4105\times10^{+002}$
Kurtosis	MBA	1.6984 (0.0361)
	LSA	2.6913
	Simulation	1.6737

computing time between the two domains: 9 min versus 30 h.

(2) Applying MBA cubicization in the proposed approach generates an accurate value of drag kurtosis with the relative error with respect to the exact 8.6667 for less than 1%.

(3) Compared with the proper results obtained from MBA approach and simulations, LSA drag cubicization causes a significant overestimation of the force kurtosis: 56% (valued around 13.51) for f_D and more than 35% for f, which in turn results in an overestimation of response kurtosis for over 50%. This can be explained by looking into the cubic polynomial coefficient that controls system nonlinearity.

(4) The contributions of the joint moments $E10$ and $E12$ are of great importance. Ignoring these two terms leads to large underestimations of kurtosis: the drag kurtosis is only around 2 and the response kurtosis is close to zero; which incorrectly implies that the response tends to be Gaussian. After all, $E10$ contains the cross-correlation among three cubic drag terms and one linear drag term, (Eq. (37)), and $E12$ has the highest-order correlation information from the cubic drag terms (Eq. (34)) They reflect the most complicated but important mechanism in formulating $R_f(\tau_1,\tau_2,\tau_3)$, albeit some 90% of computational efforts are attributable to them actually.

(5) Similar to observations in previous works, the kurtosis reduction from f to y is noticed: the Morison force kurtosis (>5.5) is much larger than that of the response (<2). The fact that the non-Gaussianity of a LTI response is weaker than that of the force excitation can be explained by the linear filtering effect of the system [6].

7. Conclusions

In this study, a correlation function-based cumulant spectral analysis method is proposed for evaluating the fourth-order cumulant function of Morison drag force without current effect. This cumulant function is expressible in terms of the autocorrelation function of water particle velocities and a complete expression needs the involvement of tenth- and twelfth-order joint moments of velocities. Three-dimensional FFT/IFFT techniques are applied to numerically estimate the trispectra of Morison force and induced response of a LTI oscillator. It is found that the force and response kurtosis obtained are in favourable agreements with those from time simulations, but with far less computational efforts. A reasonable estimation of kurtosis relies on a proper selection of the drag cubicization: the moment-based approximation is recommended.

In the presence of current where the skewness values of Morison force and response are non-zeros, the proposed cumulant spectral analysis method is still applicable to bi- and tri-spectral analyses. For an actual offshore cylinder, the excitation is the total (i.e. modal) wave force that consists of Morison forces at various underwater positions and inundation force [27]. The approach developed in this study forms a good basis, upon which the relevant discussions will be included in a separate paper.

References

[1] Liaw CY, Zheng XY. Polynomial approximations of wave loading and superharmonic responses of fixed structures. ASME J Offshore Mech Arctic Eng 2003;125(3):161–7.
[2] Borgman LE. Spectral analysis of ocean wave forces on piling. ASCE J Waterways Harbours Div 1967;93(WW2):129–56.
[3] Gudmestad OT, Connor JJ. Linearization methods and the influence of current on the nonlinear hydrodynamic drag force. Appl Ocean Res 1983;5(4):184–94.
[4] Naess A, Yim CSS. Stochastic response of offshore structures excited by drag forces. ASCE J Eng Mech 1996;122(5):442–8.
[5] Tung CC. Effects of free surface fluctuation on total wave forces on cylinder. ASCE J Eng Mech 1995;121(2):274–80.
[6] Koliopulos PK. Quasi-static and dynamic response statistics of linear SDOF system under Morison-type wave forces. Eng Struct 1988;(10): 24–36.
[7] Najafian G, Burrows R. Probabilistic modelling of quasi-static response of offshore structures subject to nonlinear wave loading: two approximate approaches. Appl Ocean Res 1994;(16):205–21.
[8] Pierson WJ, Holmes P. Irregular wave forces on a pile. ASCE J Waterways Harbours Div 1965;91(WW4):1–10.
[9] Hu JS. Stochastic dynamic response to nonlinear wave loading: fourth-moment analysis. ASCE J Eng Mech 1990;116(1):107–24.
[10] Winterstein SR. Nonlinear vibration models for extremes and fatigue. ASCE J Eng Mech 1988;114(10):1772–90.
[11] Bouyssy V, Rackwitz R. Polynomial approximation of Morison wave loading. ASME J Offshore Mech Arctic Eng 1997;(119):30–6.
[12] Olagnon M, Prevosto M, Joubert P. Nonlinear spectral computation of the dynamic response of a single cylinder. ASME J Offshore Mech Arctic Eng 1988;(110):278–81.
[13] Li XM, Quek ST, Koh CG. Stochastic response of offshore platform by statistical cubicization. ASCE J Eng Mech 1995;121(10): 1056–68.
[14] Tognarelli MA, Zhao JR, Kareem A. Equivalent statistical quadratization and cubicization for nonlinear systems. ASCE J Eng Mech 1997;123(5):512–23.
[15] Bendat JS. Nonlinear System Analysis and Identification from Random Data. New York: Wiley [pp. 22, (see also pages 396, 407)].
[16] Nikias CL, Petropulu AP. Higher-order spectra analysis. New Jersey: PTR Prentice Hall; 1993 [pp. 9 (see also pages 12–14, 16, 20–21, 37–38)].

[17] Borgman LE. Random hydrodynamic forces on objects. Ann Math Stat 1967;38(1):37–51.
[18] Price R. A useful theorem for non-linear devices having Gaussian inputs. IRE Trans Inf Theory 1958;I-4:69–72.
[19] Hu JS, Lutes LD. Non-Normal descriptions of Morison-type wave forces. ASCE J Eng Mech 1987;113(2):196–209.
[20] Hu JS, Dixit S. Non-Gaussian dynamic response to drag force. Seventh Inter Conf Offshore Mech Arctic Eng, Houston, Texas 1988;109–16.
[21] Tognarelli MA, Kareem A. Response analysis of ocean systems via moment-based hermite polynomialization. In: Spencer BF, Johnson EA, editors. Stochastic structural dynamics, rotterdam, 1999. p. 527–34.
[22] Bruce RL. Quasi-static response of jacket platforms subjected to non-linear wave loading. In: Battjes JA, editor. BOSS'85 behaviour of offshore structures, 2. The Netherlands: Delft; 1985. p. 899–905 [July 1–5].
[23] Jensen JJ. Dynamic amplification of offshore steel platform responses due to non-Gaussian wave loads. Mar Struct 1994;(7): 91–105.
[24] Liaw CY, Zheng XY. Least squares, moment based and hybrid polynomializations of Morison drag forces. ASCE J Eng Mech 2004; 130(3):294–302.
[25] Borgman LE. Ocean wave simulation for engineering design. ASCE J Waterways Harbours Div 1969;95(4):557–83.
[26] Zheng XY, Liaw CY. Response spectrum estimation for fixed offshore structures with inundation effect included. ASME J Offshore Mech Arctic Eng. and Artic Eng. 2004;(126):1–9.
[27] Zheng X.Y. Nonlinear Frequency-domain Analysis of Fixed Structures Subjected to Morison-type Wave Forces. PhD thesis, National Univ. of Singapore; 2003.
[28] SNAME Recommended practice for site specific assessment of mobile jack-up units (First edition). HSE, editor; Society of Naval Architects and Marine Engineers, 1994. p. 16–17, 81–96.